Atmospheric
Chemistry
and Physics

Evaluation of IASI-derived dust aerosol characteristics over the tropical belt

V. Capelle[1], A. Chédin[1], M. Siméon[1], C. Tsamalis[1,2], C. Pierangelo[3], M. Pondrom[1], C. Crevoisier[1], L. Crepeau[1], and N. A. Scott[1]

[1]Laboratoire de Météorologie Dynamique, UMR8539, CNRS/IPSL, Ecole Polytechnique, Palaiseau, France
[2]UK MetOffice, Exeter, UK
[3]Centre National d'Etudes Spatiales, Toulouse, France

Correspondence to: A. Chédin (chedin@lmd.polytechnique.fr)

Abstract. IASI (Infrared Atmospheric Sounder Interferometer)-derived monthly mean infrared (10 μm) dust aerosol optical depth (AOD) and altitude are evaluated against ground-based Aerosol RObotic NETwork of sun photometers (AERONET) measurements of the 500 nm coarse-mode AOD and CALIOP (Cloud-Aerosol Lidar with Orthogonal Polarization) measurements of altitude at 38 AERONET sites (sea and land) within the tropical belt (30° N–30° S). The period covered extends from July 2007 to June 2013. The evaluation goes through the analysis of Taylor diagrams and box-and-whiskers plots, separating situations over oceanic regions and over land. For the AOD, such an evaluation raises the problem of the difference between the two spectral domains used: infrared for IASI and visible for AERONET. Consequently, the two measurements do not share the same metrics. For that reason, AERONET coarse-mode AOD is first "translated" into IASI-equivalent infrared AOD. This is done by the determination, site by site, of an infrared to visible AOD ratio. Because translating visible coarse-mode AOD into infrared AOD requires accurate knowledge of variables, such as the infrared refractive index or the particle size distribution, quantifying the bias between these two sources of AOD is not straightforward. This problem is detailed in this paper, in particular in Appendix A. For the sites over oceanic regions, the overall AOD temporal correlation comes to 0.86 for 786 items (IASI and AERONET monthly mean bins). The overall normalized standard deviation (i.e. ratio of the standard deviation of the test data (IASI) to that of the reference data (AERONET)) is 0.93, close to the desired value of 1. Over land, essentially desert, correlation is 0.74 for 619 items and the normalized standard deviation is 0.86. This slight but significant degradation over land most probably results from the greater complexity of the surface (heterogeneity, elevation) and, to a lesser extent, to the episodic presence of dust within the boundary layer (particularly for sites close to active sources) to which IASI, as any thermal infrared sounder, is poorly sensitive, unlike AERONET. Site by site, disparities appear that are principally due to either the insufficient number of AERONET observations throughout the period considered, to the complexity of the location leading to the mixing of several aerosol types (in the case of the Persian Gulf, for example), to surface heterogeneities (elevation, emissivity, etc.), or to the use of a single aerosol model (called "MITR"). Results using another aerosol model, with a different refractive index, are presented and discussed. Concerning altitude over oceanic regions, correlation is 0.70 for 853 items and the normalized standard deviation is 0.92. A systematic bias of −0.4 km (IASI–CALIOP) is observed, with a standard deviation of 0.48 km. This result is satisfactory, considering the important differences between the two instruments (space–time coverage, definition of the altitude). Altitude results over land, essentially over deserts, are not satisfactory for a majority of sites. The smaller sensitivity of IASI to altitude compared to its sensitivity to AOD, added to the difficulties met for the determination of the AOD over land (surface heterogeneities), explain this result. Work is in progress to solve this difficulty.

We conclude that the present results demonstrate the usefulness of IASI data, which are planned to cover a long period of time, as an additional constraint to a better knowledge of the impact of aerosols on the climate system.

1   Introduction

During the past decades, determination of atmospheric aerosol characteristics from space has been carried out extensively using instruments measuring in the visible part of the spectrum. This has greatly contributed to enhancing our knowledge of the aerosol impact on the Earth radiation balance (direct effect) as well as on the clouds (albedo, lifetime) (indirect effect). However, these processes are complex as they involve the aerosol distribution (spatial, in particular vertical, and temporal), and their microphysical and optical properties (size, shape, composition, etc.). Moreover, the accuracy obtained on the atmospheric radiative effect also depends on surface characteristics (albedo, temperature). This complexity still leads to large uncertainties in the estimation of aerosol impacts on climate (Forster et al., 2007; US Climate Change Science Program, 2009; Hansen et al., 1997; Kaufman et al., 1997; Haywood and Ramaswamy, 1998; Claquin et al., 1998; Sokolik and Toon, 1999; Myhre and Stordal, 2001; Tanré et al., 2003; Yu et al., 2006; Otto et al., 2007; Müller et al., 2012; Ryder et al., 2013).

After a long period of relative lack of interest in aerosol remote sensing in the infrared (one of the earliest study is Legrand et al. (1989)), a marked growing interest in the infrared is now observed with the emergence of hyperspectral instruments, such as AIRS (Advanced Infrared Sounder) and IASI (Pierangelo et al., 2004, 2005; De Souza-Machado et al., 2006; Peyridieu et al., 2010, 2013; Klüser et al., 2011, 2012). Coarse-mode aerosols have a higher contribution to infrared radiation compared to fine-mode aerosols. Dust and sea-salt particles are the main components of the coarse mode, the latter usually remaining in the planetary boundary layer, at which altitudes infrared radiances collected at satellite level show poor sensitivity. Most of mineral dust aerosol mass is composed of particles in the coarse-size mode, thus with a potentially high optical depth in the infrared, and can be brought to high altitudes in the atmosphere, for example in the so-called Saharan Air Layer (Chiapello et al., 1995, 2005; Tsamalis et al., 2013). Consequently, the remote sensing of aerosols in the long-wave domain mostly focuses on retrievals of mineral dust properties (Pierangelo, 2013). This domain offers some unique opportunities such as nighttime aerosol observation, the determination of the aerosol layer mean altitude, or the aerosol characterization over deserts. Mineral dust is a major contributor to total aerosol loading and has been the subject of an increasing number of studies (e.g. Maher et al., 2010; Mahowald et al., 2010; Formenti et al., 2011; Shao et al., 2011; Knippertz and Todd, 2012), due,

in particular, to its potentially large contribution to atmospheric radiative forcing (Markowicz et al., 2003; Vogelman et al., 2003; Otto et al., 2007). Visible wavelengths are sensitive to both fine- and coarse-mode particles while infrared wavelengths are essentially sensitive to the coarse mode. Associating these two spectral domains should help improve our knowledge of the impact of aerosols on climate, its variability, and evolution. This requires validating infrared-derived aerosol properties using well-recognized, accurate and independent measurements of these properties, as well as understanding possible differences emerging from such comparison.

In this study, IASI-derived monthly mean dust $10\,\mu m$ AOD (aerosol optical depth), for the period July 2007–June 2013 (Peyridieu et al., 2013), is evaluated using accurate measurements, routinely made and distributed by the Aerosol RObotic NETwork of sun photometers (AERONET; Holben et al., 1998), for 38 sites in the tropical band. In this approach, use is made of the 500 nm coarse-mode AOD from the Spectral Deconvolution Algorithm (SDA) (O'Neill, 2003). Then, at the same 38 AERONET sites, IASI-derived altitude is evaluated using observations of the two-wavelength depolarization lidar CALIOP onboard the satellite CALIPSO (Winker et al., 2007).

IASI, AERONET, and CALIOP data are described in Sect. 2. Section 3 describes the method followed for evaluating IASI results, based on the use of Taylor diagrams (Taylor, 2001) and box-and-whiskers plots. Section 4 presents the results of the evaluation. In this section, the impact of the choice of an infrared refractive index model made in this study is also discussed. Results of this evaluation are discussed in Sect. 5.

2   Data

2.1   IASI

Developed by CNES (Centre National d'Etudes Spatiales) in collaboration with EUMETSAT (European Organization for the Exploitation of Meteorological Satellites), the IASI instrument (Chalon et al., 2001; http://smsc.cnes.fr/IASI), onboard the Metop-A polar platform, is a Fourier transform spectrometer that measures Earth-emitted infrared radiation. Launched in October 2006 and operational since July 2007, it provides 8461 spectral channels, between $15.5\,\mu m$ ($645\,cm^{-1}$) and $3.63\,\mu m$ ($2755\,cm^{-1}$), with a spectral resolution of $0.50\,cm^{-1}$ after apodization, and a regular spectral sampling interval of $0.25\,cm^{-1}$. Metop-A crosses the Equator at 21:30 LT, on its ascending node. IASI provides a near global coverage twice a day at a spatial resolution of 12 km at nadir. The period covered by the present study ranges from July 2007 to June 2013.

The method used to derive dust characteristics from IASI observations is a three-step algorithm based on a

"Look-Up-Table" (LUT) approach (Pierangelo et al., 2004, 2005; Peyridieu et al., 2010, 2013). The first step determines the atmospheric state observed; the second step simultaneously determines the 10 μm AOD and the aerosol layer mean altitude while the dust coarse-mode effective radius is determined in the third step. It is worth pointing out that, measuring in the infrared, IASI is essentially sensitive to the dust coarse mode, with a sensitivity to the fine mode of about 10 % or less. The dust model used is the "mineral transported" (MITR) aerosol model from the "Optical Properties of Clouds and Aerosols" (OPAC) database (Koepke et al., 1997; Hess et al., 1998). The main microphysical parameters associated with this model are: a monomodal lognormal distribution with a mode radius of 0.5 μm (r_{modN}), standard deviation of the size distribution equalling 2.2 ($\ln\sigma_g = 0.78$), and particle density of 2.6 g cm^{-3}. At 10 μm, the corresponding optical parameters are mass extinction efficiency of 0.24 m^2 g^{-1}, single scattering albedo of 0.48, asymmetry factor of 0.44. Look-Up-Tables of IASI-simulated brightness temperatures are calculated using the forward-coupled radiative transfer model 4A/OP-DISORT (Scott and Chédin, 1981; Stamnes et al., 1988; http://4aop.noveltis.com). Entries to the model include AOD, altitude, surface pressure, surface temperature and emissivity, viewing angle, and a set of about 600 atmospheric situations representative of the tropical band (30° S–30° N). Over land, surface spectral emissivity is taken from Capelle et al. (2012). IASI observations are processed spot by spot (daily), averaged monthly, and gridded 1° by 1°. Several aspects of the retrieval algorithm such as the robustness to aerosol model (size distribution, shape, and refractive index), the possible contamination by other aerosol species, the radiative transfer model bias removal, or the cloud mask including discrimination between clouds and aerosols, etc., were investigated in Pierangelo et al. (2004) and in Peyridieu et al. (2010).

2.2 AERONET

Accurate ground-based measurements are essential to evaluating satellite-derived aerosol characteristics. Here, we use the measurements routinely made and distributed by the AERONET (Holben et al., 1998), particularly the SDA retrieval of the coarse-mode AOD monthly averages. Indeed, as explained by O'Neill (2003), recognising that the aerosol particle size distribution is effectively bimodal permits the extraction of the fine- and coarse-mode optical depths from the spectral shape of the total aerosol optical depth. Comparison between infrared spaceborne and visible ground-based instruments requires keeping in mind that the IASI observations used here are made at nighttime at 21:30 LT, while AERONET measures during daytime; this difference should not be too important on a monthly scale, except in the presence of a strong, well-established, local diurnal cycle affecting the free troposphere. A total of 38 AERONET sites have been selected within the tropical belt, both over oceanic
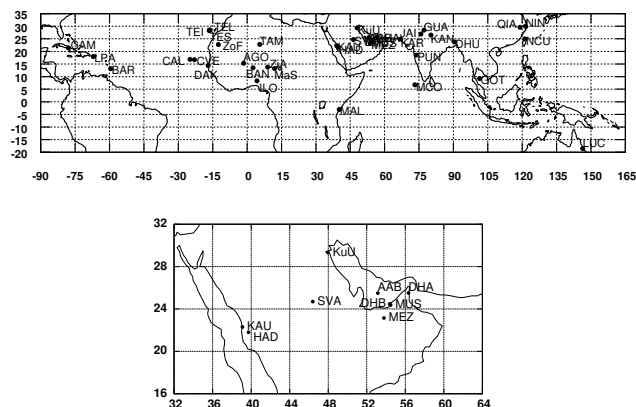

Figure 1. Location of the 38 AERONET sites selected for this study. Top: whole tropical belt; bottom: zoom of the Arabian Peninsula. See Table 1 for the meaning of the three-letter codes.

regions (coasts or islands) and over land. Four coastal sites are used both over land and sea which means that AERONET measurements are associated with IASI data either over oceanic regions or over land. This selection takes into account the availability of a sufficient number of items ("items" refers to IASI and AERONET monthly mean bins throughout the paper) throughout the time period studied: from July 2007 to June 2013, a maximum of 72 items may be expected; a few sites, representative of a region of interest, with less than 12 items (6 sites over oceanic regions and 1 over land) have however been kept. To provide a sufficiently large and representative list of sites, the coarse-mode AERONET AOD is of quality "Level 1.5" for a minority of sites (15) selected, meaning that they have been cloud-screened but may not have final calibration applied; the other sites are of quality "Level 2.0" (quality-assured). Table 1 lists the 38 AERONET sites: name, longitude, latitude, three-letter code, elevation (in m), and 500 nm coarse-mode AERONET AOD data quality level. Figure 1 shows the location of each AERONET site selected for this study: the top shows the whole tropical belt and the bottom is a zoom on the Arabian Peninsula for the sake of readability. Out of all the sites listed in Table 1, the 9 first sites are located in the Persian Gulf or in the Arabian Peninsula, the following 9 are over Africa, the following 8 over the Atlantic Ocean, and the following 11 over Asia; the last site is located over Australia.

2.3 CALIOP

Launched in April 2006, the satellite CALIPSO with the on board two-wavelength depolarization lidar CALIOP permits an accurate determination of the aerosol altitude (Winker et al., 2009, 2010) to which IASI-derived altitude is here compared. CALIOP, a near-nadir viewing instrument, has a very narrow swath (beam diameter of 70 m at the Earth's surface, giving a 16-day repetition cycle). Actually, rarely more than two to three collocations between IASI and CALIOP can

Table 1. List of the 38 AERONET sites selected for this study: name, longitude (degree), latitude (degree), three-letter code, elevation (in m), 500 nm coarse-mode AOD data quality level.

Site	Long	Lat	Code	Z(m)	Q Lev
Abu_Al_Bukhoosh	53.146	25.495	AAB	24	1.5
Dhabi	54.383	24.481	DHB	15	2.0
Dhadnah	56.325	25.513	DHA	81	2.0
Kuwait_University	47.971	29.325	KuU	42	2.0
Mezaira	53.779	23.145	MEZ	204	2.0
Mussafa	54.467	24.372	MUS	10	2.0
Solar_Village	46.397	24.700	SVA	764	2.0
Hada_el-Sham	39.729	21.802	HAD	254	1.5
KAUST_Campus	39.102	22.304	KAU	11	2.0
Agoufou	−1.479	15.345	AGO	305	1.5
Banizoumbou	2.665	13.541	BAN	250	1.5
Dakar	−6.959	14.394	DAK	0	2.0
DMN_Maine_Soroa	12.023	13.217	MaS	350	1.5
Tamanrasset_INM	5.530	22.790	TAM	1377	2.0
Zinder_Airport	8.990	13.777	ZiA	456	1.5
Zouerate-Fennec	−12.483	22.750	ZoF	343	1.5
Ilorin	4.340	8.320	ILO	350	2.0
CRPSM_Malindi	40.194	−2.996	MAL	12	1.5
Calhau	−24.867	16.864	CAL	40	1.5
Camaguey	−77.850	21.422	CAM	122	2.0
Capo_Verde	−22.935	16.733	CVE	60	2.0
Santa_Cruz_Tenerife	−16.247	28.473	TES	52	2.0
Izana	−16.499	28.309	TEI	2391	2.0
La_Laguna	−16.321	28.482	TEL	568	2.0
La_Parguera	−67.045	17.970	LPA	12	2.0
Ragged_Point	−59.432	13.165	BAR	40	2.0
Karachi	67.030	24.870	KAR	49	2.0
MCO-Hanimaadhoo	73.183	6.776	MCO	0	2.0
Pune	73.805	18.537	PUN	559	1.5
Jaipur	75.806	26.906	JAI	450	2.0
Gual_Pahari	77.150	28.426	GUA	384	2.0
Kanpur	80.232	26.513	KAN	123	2.0
Dhaka_University	90.398	23.728	DHU	34	1.5
GOT_Seaprism	101.412	9.286	GOT	10	1.5
Qiandaohu	119.053	29.556	QIA	133	1.5
EPA-NCU	121.185	24.968	NCU	144	2.0
Ningbo	121.547	29.860	NIN	121	1.5
Lucinda	146.386	−18.520	LUC	8	1.5

be observed during 1 month in the tropics. For that reason, starting from the L2 5 km aerosol layer product (version 3), monthly mean CALIOP altitudes are calculated at a resolution of $3° \times 3°$ following the approach and quality criteria of Tsamalis et al. (2013). It is worth recalling that the altitudes seen by either IASI or by CALIOP do not have the same definition. For IASI, altitude is "infrared equivalent" altitude, i.e. the altitude at which half of the dust optical depth is below and half of the optical depth is above, while, for CALIOP, it is the mean value calculated from the vertical distribution of dust occurrence frequency (see Tsamalis et al. (2013) for details), thus independent from the dust load. The CALIOP mean altitude is calculated in this way in order to avoid the critical influence of the lidar ratio on the estimation of the extinction coefficient (and the optical depth), and the possible misclassification of dust layers as polluted dust, which affects the assignment of the lidar ratio. These issues, already

discussed in Tsamalis et al. (2013), are related to the fact that CALIOP is an elastic lidar, meaning that it needs an assumption about the lidar ratio to retrieve the extinction coefficient. Recent studies further corroborate our choice by finding significant AOD differences between CALIOP and other instruments (Amiridis et al., 2013; Ma et al., 2013; Omar et al., 2013; Tesche et al., 2013). Moreover, IASI shows low sensitivity to a complex layering of the dust (Pierangelo et al., 2004).

3 Method

IASI monthly mean $1° \times 1°$ gridded AOD and altitude are first averaged over boxes centred around each AERONET site. A large majority of the boxes ($\sim 70\%$) are of the size $\pm 1.5°$ by $\pm 1.5°$. Over land, in particular, this standard box size may vary slightly according to the characteristics of the terrain (presence of high orography, of lakes, of a complex coastal configuration, etc.). For each site, all pairs of monthly mean AOD from IASI, provided it is larger than 0.02 (a limit imposed by the IASI sensitivity to AOD) and from AERONET, available over the period considered, are included in the evaluation; the same rule applies for IASI and CALIOP altitude, provided IASI altitude is larger than 1 km. In the following such a data pair will be referred to as one item.

To quantify how accurately IASI agrees with AERONET or CALIOP, use is made here of a Taylor diagram approach (Taylor, 2001). As explained by the author, this diagram can concisely summarize how well two patterns match each other in terms of their correlation, their root-mean-square (rms) difference, and the ratio of their variances (or standard deviations). Here, the two patterns are IASI (AOD or altitude) on the one hand, and AERONET for the AOD or CALIOP for the altitude on the other. In this diagram, the correlation coefficient and the rms difference between the two fields, along with the ratio of the standard deviations of the two patterns, are all indicated by a single point. In the following, we use the "normalized" version of the Taylor diagram, which means that the rms difference and the two standard deviations (one for each pattern) have been normalized by the standard deviation of the corresponding reference field, here AERONET for the AOD or CALIOP for the altitude.

Moreover, because the diagram has been designed to convey information about centred pattern differences, we also use box-and-whiskers plots to characterize the distributions of the differences between the two patterns considered. This approach is important in that such box plots display differences between populations without making any assumptions about the underlying statistical distribution. The plots presented here show the first and third quartiles and the median, the ends of the whiskers being the minimum and maximum of all of the data remaining after elimination of "outliers" (see below).

For the AOD, such a comparison raises the problem of the difference between the two spectral domains used: infrared (IASI) and visible (AERONET). Assuming a monomodal size distribution in the two cases (the contribution of the fine mode to the IASI AOD is ∼ 10 % or less; Pierangelo, 2013), the infrared (IR; 10 μm) / visible (Vis; 500 nm) AOD coarse-mode ratio essentially depends on the refractive index, on the width of the size distribution, and on the effective radius. Because the parameters involved in the determination of the ratio vary from one site to another (and possibly throughout the time period for a given site), there is no one common factor reconciling the two observation metrics. To overcome this difficulty, a fit is done, site by site, including all the available items over the period studied, resulting in an IR (10 μm) / Vis (500 nm) AOD coarse-mode "empirical" site ratio. As detailed in Appendix A, a theoretical site ratio can be estimated from the a priori knowledge of the aerosol microphysical properties (size distribution and effective radius, refractive index), using a Lorenz–Mie calculation (see, for example, Mishchenko et al., 2002). Results show that the theoretical ratio strongly varies with both the size distribution (Fig. A3, left) and the refractive index (Fig. A3, right). For typical values of the effective radius and width of the size distribution from AERONET, the theoretical ratio may vary between 0.6 and 1.3. However, being provided by the AERONET database at each site studied, these two parameters are not a real problem for the evaluation of IASI. Regarding the refractive index, the theoretical ratio, estimated using the microphysical properties measured by AERONET, may vary from 0.4 for aerosol close to sources to 1.1 for aerosols transported far from the sources (see Appendix A for details). This is a very large range of variation: assuming a different refractive index model can lead to quite a different theoretical site ratio. As a consequence, assuming a wrong refractive index leads directly to a bias between IASI infrared and AERONET visible AOD. The lack of knowledge of the true infrared refractive index model to use at each site explains our choice of determining "empirical" IR / Vis AOD coarse-mode site ratios through a fitting procedure. The problem associated with this method is that of a bias potentially affecting the IASI AOD (or AERONET coarse-mode AOD): in this case, the procedure will mask the bias and produce a wrong empirical site ratio. As discussed in the following (Sect. 4.1), results of the site-by-site empirical fits are within the range of variation of their theoretical values and, also, in reasonable agreement with values from Highwood et al. (2003). In addition to leading to wrong empirical site ratios, the presence of biases should affect the amplitude of the seasonal cycles as well as degrade the correlation. Both sets of information are given and discussed site by site; they should help assess the quality of the retrieved IASI AOD. In the remainder of the paper, for each AERONET site, the visible coarse-mode AOD is multiplied by the empirical site ratio prior to being compared to IASI infrared AOD.

Finally, all statistical results are given after having eliminated so-called "outliers" for which the difference between the IASI and the reference data stands too far from the mean of all the sites. Here, the test distance has been chosen so that about 7 % of the items are eliminated. Outliers may correspond to remaining thin clouds not detected by the cloud detection algorithm, to strong temporal aerosol heterogeneities (bearing in mind that IASI and AERONET, and a fortiori CALIOP, do not often measure the same days in the month), to limits of the IASI retrieval algorithm, or to errors in the AERONET (AOD) or CALIOP (altitude) observations. This procedure allows us to eliminate cases which would otherwise mask the real performance of the evaluation.

4 Results

A few remarks are necessary to explain the analysis below. First, the signal induced on IASI observations by each variable of interest, here AOD or altitude, depends on its magnitude. This is, however, less trivial for the altitude but, generally, the higher the altitude the larger the signal. This is due to the decreasing thermal contrast between the surface and the atmosphere when approaching the surface. Hence, infrared sounders show a limited sensitivity to the boundary layer. Second, the signal induced by altitude is intrinsically smaller than that induced by AOD: retrieving accurate altitude is, therefore, more difficult, even more so for low AOD. Third, IASI, a remarkably accurate and stable instrument, has a drawback in that the larger noise of its short wavelength channels prevents good disentangling of the AOD and altitude signals; this difficulty has more impact on the altitude than on the AOD.

4.1 Evaluation of IASI 10 μm AOD

In the following, for the sake of a simpler identification, each site name is followed by a parenthesized number referring either to Table 2 for sites over oceanic regions or to Table 3 for sites over land. As mentioned previously, a few sites are used both over oceanic regions and over land which means that AERONET measurements are associated with IASI data either over oceanic regions or over land. This is the case for Dakar, Karachi, Pune, and Solar_Village, the latter, an obvious land site, for reasons discussed below.

4.1.1 IR / Vis AOD coarse-mode site ratios

IR / Vis AOD coarse-mode ratios have been computed for all the sites, over oceanic regions and over land, as explained in Sect. 3. It is important to point out that the quality of the fit for each site will depend on the number of items available (as said above, a maximum of 72 items in 6 years may be expected). Sites with obviously not enough items to correctly represent the seasonal cycle may lead to a wrong site ratio. For that reason, site ratio statistics exclude those sites with

Table 2. Correlation between IASI AOD and 500 nm coarse-mode AERONET AOD (column 5), and amplitude (normalized standard deviation of IASI) (last column), over oceanic regions. Each site is identified by its name (first column), its three-digit code (second column), and identification number (third column). The fourth column gives the number of items in the statistics ("Nb it"). The last line gives the overall statistics (all sites merged). An asterisk in the first column indicates that the AERONET coarse-mode AOD data at this site are "Level 1.5" instead of "Level 2.0" (see text). Bold names correspond to stations with weak mean IASI AOD (all-period average less than 0.08).

Site	Code	No.	Nb It	Correl.	Amplit.
Abu_Al_Bukhoosh*	AAB	1	12	0.67	0.82
Dhabi	DHB	2	7	0.87	0.68
Dhadnah	DHA	3	23	0.70	0.67
Kuwait_University	KuU	4	23	0.74	0.83
Mussafa	MUS	5	15	0.62	0.74
Solar_Village	SVA	6	52	0.83	0.89
KAUST_Campus	KAU	7	10	0.78	1.77
CRPSM_Malindi*	MAL	8	42	0.51	1.44
Calhau*	CAL	9	14	0.75	0.77
Camaguey	CAM	10	31	0.91	1.05
Capo_Verde	CVE	11	65	0.85	0.86
Dakar	DAK	12	35	0.73	0.65
Santa_Cruz_Tenerife	TES	13	51	0.82	1.04
Izana	TEI	14	55	0.85	0.93
La_Laguna	TEL	15	39	0.89	1.05
La_Parguera	LPA	16	43	0.86	0.93
Ragged_Point	BAR	17	59	0.71	0.99
Karachi	KAR	18	59	0.91	0.99
MCO-Hanimaadhoo	MCO	19	34	0.60	0.90
Pune*	PUN	20	50	0.81	1.03
Dhaka_University*	DHU	21	10	0.85	0.96]
GOT_Seaprism*	GOT	22	9	0.54	1.08
EPA-NCU	NCU	23	36	0.62	0.72
Ningbo*	NIN	24	5	0.85	0.85
Lucinda*	LUC	25	8	0.67	1.11
All sites merged	av		786	0.86	0.93

Table 3. Same as for Table 2 except over land.

Site	Code	No.	Nb it	Correl.	Amplit.
Mezaira	MEZ	1	39	0.55	0.57
Solar_Village	SVA	2	55	0.47	0.84
Hada_el-Sham*	HAD	3	8	0.50	0.35
Agoufou*	AGO	4	39	0.64	0.65
Banizoumbou*	BAN	5	65	0.60	0.81
Dakar	DAK	6	35	0.74	0.77
DMN_Maine_Soroa*	MaS	7	28	0.55	0.59
Tamanrasset_INM	TAM	8	14	0.87	0.71
Zinder_Airport*	ZiA	9	47	0.53	0.52
Zouerate-Fennec*	ZoF	10	15	0.76	0.41
Ilorin	ILO	11	47	0.53	0.82
Karachi	KAR	12	62	0.78	0.62
Pune*	PUN	13	49	0.77	0.89
Jaipur	JAI	14	32	0.88	0.56
Gual_Pahari	GUA	15	12	0.82	0.89
Kanpur	KAN	16	56	0.61	0.85
Qiandaohu*	QIA	17	12	0.51	1.32
All sites merged	av		619	0.74	0.85

4.1.2 Evaluation of IASI 10 μm AOD over oceanic regions

Table 2 gives the correlation (column 5), site by site, obtained between IASI and 500 nm coarse-mode AERONET AOD, and the normalized standard deviation of IASI (last column). In the following, the normalized standard deviation will be referred to as "amplitude", as often representative of the amplitude of the seasonal cycle. For each site, identified by its full name, three-digit code, and number (columns 1, 2, and 3, respectively), the number of items in the statistics is also given. The last line of this table gives the overall statistics. Sites marked by an asterisk indicate that the AERONET coarse-mode AOD at this site is "Level 1.5" instead of "Level 2.0" (see Sect. 2.2). 32 % of the sites considered are concerned. Bold names correspond to sites for which the full-period averaged IASI AOD is less than 0.08, noting that a majority of sites have an averaged AOD of the order of 0.15 (see also the AOD time series in the Supplement). With a total of 786 items and overall correlation of 0.86, one may reasonably conclude that IASI matches AERONET well. Suppressing the elimination of outliers leads to an overall correlation of 0.78 for 853 items. Site by site, disparities appear with, for example, CRPSM_Malindi(8) and a weaker correlation of 0.51; this is mainly due to the small IASI AOD observed throughout the period (average AOD of 0.04) at or even under the limit of the method and is perhaps also due to the quality "Level 1.5" of this site. However, other "Level 1.5" sites show good correlation as, for example, Pune(20) or Dhaka_University(21) with 0.81 and 0.85, respectively.

Figure 2 shows the Taylor diagram (normalized by the reference AERONET) for the IASI and the AERONET coarse-mode AOD. In this figure, the labels (numbers) correspond to those in Table 2 and the symbol "av" stands for the result
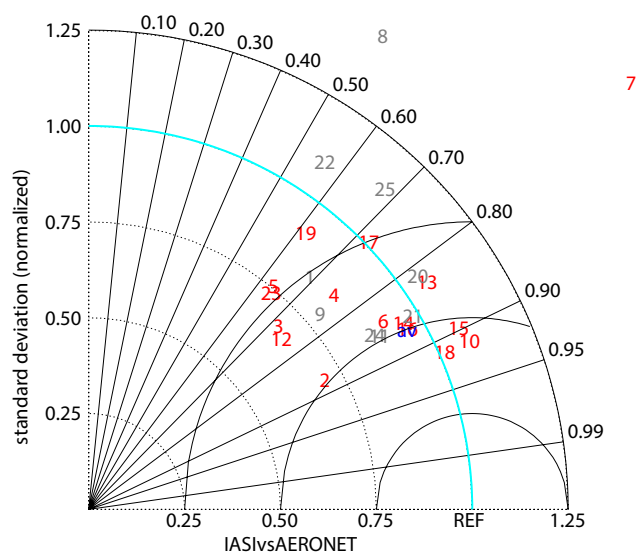
less than 20 items. The site of Izana, measured at an altitude of ∼ 2.4 km, is also excluded. Averaged over all remaining sites, the mean ratio comes to 0.79 ± 0.25 for the sites over oceanic regions and to 0.55 ± 0.15 for the sites over land. The fact that the mean site ratio is larger over oceanic regions, where the MITR aerosol model seems best adapted, than over land, where the "dust-like" or "Volz–Fouquart" model is a priori better adapted, agrees with the theory (see Appendix A). One may also note the slightly (in percent) larger standard deviation for the sites over oceanic regions compared to the sites over land. This may be due in part to the label "sea" given to sites far from the aerosol sources as well as to sites, e.g. in the Persian Gulf, closer to sources. This is also due to the two Tenerife sites (TEL and TES), both showing ratios much larger (∼ 1.2) than the mean. Kalashnikova and Kahn (2008) had already observed the particular behaviour of these sites, which is still not clearly understood.

Figure 2. Taylor diagram (normalized) for IASI and AERONET 500 nm coarse-mode AOD over oceanic regions. Sites are identified by their number in Table 2. Grey numbers are for "Level 1.5" sites. The overall statistics appear in blue ("av" for average). Correlation shown on the external circle; amplitude: radial distance.

Figure 3. Box-and-whiskers plot (ends of the whiskers exclude the outliers) for the difference between IASI and AERONET 500 nm coarse-mode AOD (scaled by the site ratio as explained in Sect. 3) over oceanic regions. Sites are identified by their number and code in Table 2, followed by the number of items. Last box marked "Tot": overall result.

obtained when all items from the 25 sites over oceanic regions are merged. In addition to the good overall correlation of 0.86 already seen, this diagram provides an overall ("av") amplitude of 0.93, similar to that of the AERONET reference, marked by the cyan arc indicating a radius of 1. Four sites, located far from aerosol sources, Camaguey(10), Capo_Verde(11), La_Parguera(16), and Ragged_Point(17), show an amplitude close to 1, with good correlations. Three sites of the Persian Gulf (Dhabi(2), Dhadnah(3), Mussafa(5)), and Dakar(12), which are relatively close to aerosol sources, show smaller amplitudes (by about 25 %). For Dhabi(2) and Mussafa(5) to a lesser extent, the number of items is among the smallest. For these sites, the MITR model is probably not adapted well enough. CRPSM_Malindi(8), with a weak correlation, shows a much larger amplitude (1.4) compared to the reference than KAUST_Campus(7) with an amplitude of 1.8 (and a better correlation of 0.78). Results for sites, such as GOT_Seaprism(22), Ningbo(24), or Lucinda(25), are not really significant, probably due to their low numbers of items; see Table 2. These differences may, at least partially, be due to the way the AERONET metrics are adapted to the IASI metrics (see Sect. 3). As already explained in Sect. 3, biases affecting IASI AOD as well as too few AERONET measurements, poorly distributed throughout the time period studied, can degrade the fit, leading to a wrong IR / Vis coarse-mode AOD ratio. The correlation is weak for the two sites MCO-Hanimaadhoo(19) and EPA-NCU(23). Both are under the influence of a variety of aerosol sources, as revealed by trajectory analysis (Eck et al., 2001; Wang et al., 2010). They are also sites where conditions make
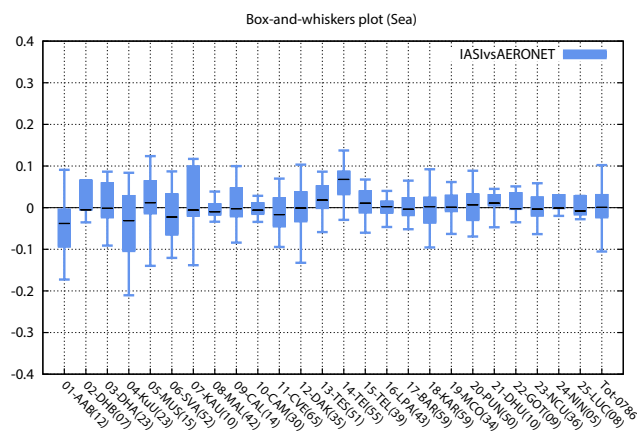
the MITR aerosol model inappropriate; this problem is discussed in Sect. 4.3.

Figure 3 shows the box-and-whiskers plot for the difference between IASI and AERONET AOD: first and third quartiles and median. The ends of the whiskers are the minima and maxima of all of the data, outliers excluded. For the overall sample, there is almost no skewness and a relatively small inner quartile range (third quartile minus first quartile) of ∼ 0.05. Most sites show a small skewness with the noticeable exception of Izana(14), but the altitude of this site is ∼ 2400 m (see also Sect. 3), and of the sites with too small a number of items (Dhabi(2), KAUST_Campus(7), Dhaka_University(21), etc.), which actually display dubious results as far as the data distribution is concerned. For the sites with more items available, poor results may indicate the use of a wrong IR / Vis coarse-mode AOD ratio (see above).

4.1.3 Evaluation of IASI 10 μm AOD over land

As in Table 2 for the sites over oceanic regions, Table 3 gives the correlation (column 5) obtained between IASI and the 500 nm coarse-mode AERONET AOD and the amplitude (last column). Here, the overall correlation reaches 0.74 for 619 items (0.67 for 660 items without elimination of the outliers), a relatively good result keeping in mind that, here, the proportion of "Level 1.5" sites (marked by an asterisk) is larger than over oceanic regions (47 %). The overall amplitude (0.86) is significantly lower than for the sites over oceanic regions (0.93). This is also due to the use of the MITR model for sites close to aerosol sources. As for the sites over oceanic regions, site by site disparities appear with, for example, the high correlation (0.87) of Tamanrasset_INM (8), however, for which there are only 14 items available, or the weak correlation (0.47) of Solar_Village(2). This poor
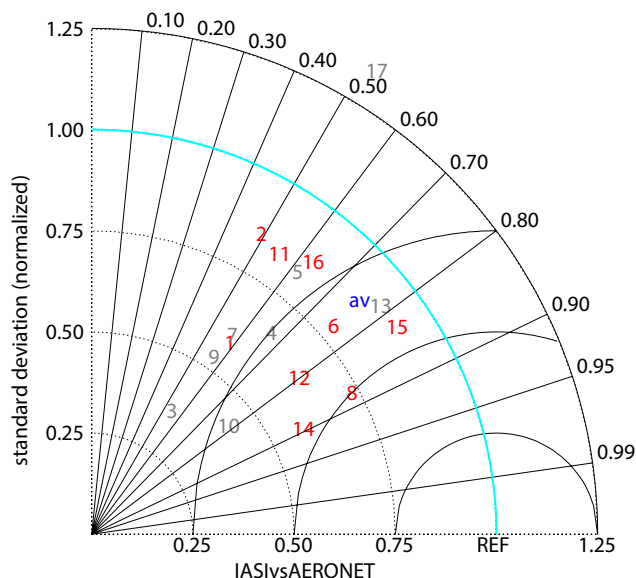
Figure 4. Same as for Fig. 2 except over land. Sites are identified by their number in Table 3.

Figure 5. Box-and-whiskers plot (ends of the whiskers exclude the outliers) for the difference between IASI and AERONET 500 nm coarse-mode AOD (scaled by the site ratio as explained in Sect. 3) over land. Sites are identified by their number and code in Table 3, followed by the number of items. Last box marked "Tot": overall result.

correlation for a site with a relatively high number of items (55) has at least two explanations: terrain heterogeneities and elevation (about 850 m). This situation complicates the retrieval of AOD by rendering channels sensitive to the lower part of the atmosphere even more transparent and hence more affected by surface heterogeneities. As a consequence, errors in the surface emissivity and/or temperature have larger consequences. This has led us to associate Solar_Village AERONET measurements with IASI data from the nearest region (centred at 27° N, 51° E; box of ±1° in latitude and longitude), over oceanic regions of the Persian Gulf, bearing in mind the prevalence of roughly similar weather conditions over the Arabian Peninsula during the pre-monsoonal (spring) and monsoonal (summer) period, when maximum dust activity occurs (Walters Sr. and Sjoberg, 1990; Smirnov et al., 2002; Léon and Legrand, 2003). This time, a strong correlation of 0.83 is obtained as seen in Table 2 and Fig. 3. We see this result as a confirmation of the increased difficulty in retrieving aerosol characteristics over "difficult" terrains. Except Zouerate-Fennec(10) and Pune(13), all other "Level 1.5" sites show relatively weak correlations.

Figure 4 shows the Taylor diagram (normalized by the reference AERONET) for IASI and AERONET coarse-mode AOD. The largest discrepancies, marked by a much too low amplitude compared to AERONET, can be seen at three "Level 1.5" sites (Hada_el_Sham(3), Zinder_Airport(9), and Zouerate_Fennec (10)), although the latter shows a strong correlation; however, Pune(13), also a "Level 1.5" site, shows good results. Among the "Level 2" sites, Tamanrasset_IMN(8) shows a strong correlation but too low an amplitude (∼ 0.75), Gual_Pahari(15) has good results, and Solar_Village(2) has the weakest correlation and an amplitude
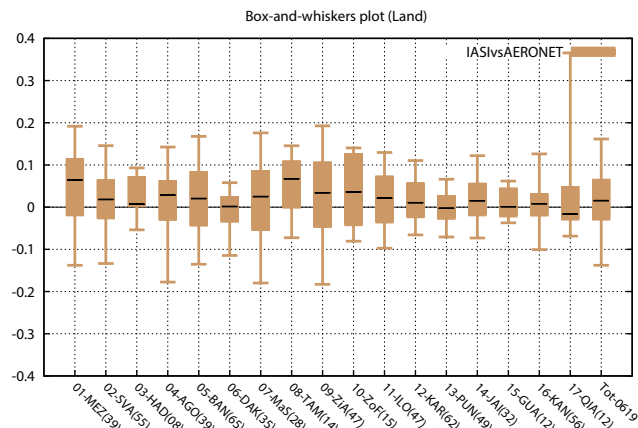
too low by ∼ 20 % (note that, as an "over oceanic regions" site, its amplitude is almost equal to 1; see Fig. 3). The amplitude corresponding to the whole ensemble of items from the 17 merged overland sites ("av" on the graph) is slightly smaller (13 %) than that of the reference (AERONET). Actually, all sites show a deficit, but some of them (Mezaira(1), Karachi(12), Jaipur(14)) more than the others. This is all the more true over Sahara, most sites being "Level 1.5". These results confirm that the MITR model is not well adapted to these situations closer to sources. They also show that the presence of pronounced terrain heterogeneities has a negative impact on the accuracy of the AOD retrieved from IASI, this being due to the increased difficulty in determining surface characteristics (emissivity and temperature; see Capelle et al., 2012).

Figure 5 shows the box-and-whiskers plot for the difference between IASI and AERONET AOD: first and third quartiles and median for the sites over land. Results are significantly worse than over oceanic regions, with a majority of skewed distributions, most pronounced for Mezaira(1) and Tamanrasset_IMN(8), the latter with only 14 items (and an elevation of ∼ 1400 m). As a consequence, the overall distribution is slightly skewed and the ends of the whiskers are at about ±0.15 instead of ±0.1 over oceanic regions.

Both over oceanic regions (coastal) and over land, the sites in the Middle East are not among the best, with a few exceptions. This might be due to the aerosol heterogeneity in this region (Kaskaoutis et al., 2010), where coarse-mode desert dust aerosols often mix with fine-mode pollution aerosols largely produced by the petroleum industry and themselves possibly affected by aerosol humidification growth (Smirnov et al., 2002; Eck et al., 2008; Reid et al., 2005, 2006, 2007, 2008; Basart et al., 2009). This is somewhat similar for

Table 4. Correlation between IASI and CALIOP altitude (column 5) and amplitude (last column) over oceanic regions. Each site is identified by its name (first column), its three-digit code (second column), and identification number (third column). The fourth column gives the number of items in the statistics. The two last lines give the overall statistics: first line – all sites merged; second line – without three sites (Malindi, Ningbo, Lucinda), see text.

Site	Code	No.	Nb it	Correl.	Amplit.
Abu_Al_Bukhoosh	AAB	1	40	0.62	1.28
Dhabi	DHB	2	40	0.62	1.28
Dhadnah	DHA	3	45	0.75	1.18
Kuwait_University	KuU	4	44	0.65	1.07
Mussafa	MUS	5	43	0.76	1.23
Solar_Village	SVA	6	43	0.79	1.11
KAUST_Campus	KAU	7	45	0.80	0.86
CRPSM_Malindi	MAL	8	42	0.23	0.18
Calhau	CAL	9	47	0.78	1.09
Camaguey	CAM	10	22	0.10	1.05
Capo_Verde	CVE	11	47	0.78	1.09
Dakar	DAK	12	47	0.83	1.59
Santa_Cruz_Tenerife	TES	13	42	0.63	0.58
Izana	TEI	14	42	0.63	0.58
La_Laguna	TEL	15	42	0.63	0.58
La_Parguera	LPA	16	24	0.61	1.29
Ragged_Point	BAR	17	27	0.64	1.14
Karachi	KAR	18	47	0.65	0.51
MCO-Hanimaadhoo	MCO	19	43	0.82	0.88
Pune	PUN	20	45	0.78	0.74
Dhaka_University	DHU	21	38	0.57	0.39
GOT_Seaprism	GOT	22	27	0.24	1.61
EPA-NCU	NCU	23	30	0.52	0.25
Ningbo	NIN	24	14	0.03	0.48
Lucinda	LUC	25	14	−0.52	0.23
All sites merged	av	929		0.65	0.91
All sites (filtered)	av	853		0.70	0.92

Figure 6. Taylor diagram (normalized) for IASI and CALIOP altitude over oceanic regions. Sites are identified by their number in Table 4. The overall statistics appear in blue ("av" for average).

Ilorin(11) and Kanpur(16) (Singh et al., 2004; Eck et al., 2010). One may note that the "Global dust model intercomparison in AeroCom Phase I" (Huneeus et al., 2011) came to similar conclusions for the Middle East AERONET stations and the coarse-mode AOD. More generally, results over land are significantly worse than over oceanic regions, the main reasons being (i) the use of the MITR model, particularly its refractive index in the infrared (see Appendix A), for sites close to aerosol sources; (ii) the greater complexity of the surface (heterogeneities, elevation); and (iii), the episodic presence of dust in the lower troposphere, particularly for sites close to active sources (the Sahara, for example), to which IASI is poorly sensitive, unlike AERONET. Close to sources, the measurement time difference between IASI (at night) and AERONET may also be a problem due to the presence of a diurnal cycle (Kocha et al., 2013).

4.2 Evaluation of IASI altitude over oceanic regions

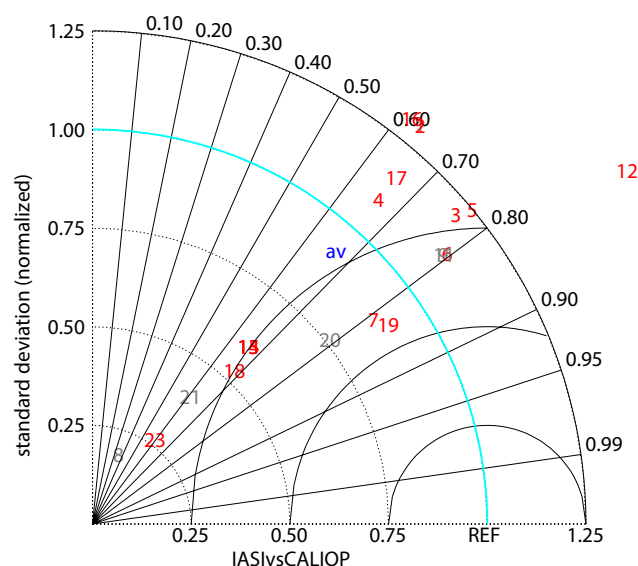As in Table 2 for the AOD, Table 4 gives the correlation (column 5) obtained between IASI and CALIOP altitude and the amplitude (last column). Overall statistics with all sites merged give a correlation of 0.65 for 929 items and an overall amplitude of 0.91. Eliminating three sites – CRPSM_Malindi(10), due to too low a mean AOD (0.04), and Ningbo(24) and Lucinda(25), due to too low a number of items (14) – gives a correlation of 0.7 for 853 items (overall amplitude: 0.92). These weaker correlations, compared to the AOD, had to be expected due to (i) the sensitivity of IASI, lower to altitude than to AOD (Pierangelo et al., 2004); (ii) the different definitions of the two altitude products (see Sect. 2.3); and (iii) the large differences in the space–time resolution of IASI and CALIOP. Here again, site by site disparities appear with, for example, sites far from the sources characterized by a weak AOD throughout the time period (see Table 2, bold face sites). CRPSM_Malindi(8), Camaguey(10), La_Parguera(16), Ragged_Point(17), GOT_Seaprism(22), EPA-NCU(23), or Lucinda(25) are examples of such sites, showing a low correlation. This is due to the fact that a low AOD increases the difficulty of determining the altitude from IASI (there are a few exceptions: MCO-Hanimaadhoo(19) or Pune(20), which show strong correlations of 0.82 and 0.78, respectively). Sites, such as Calhau(9) or Capo_Verde(11), or some sites of the Persian Gulf, closer to sources, show better correlations.

Figure 6 shows the Taylor diagram for IASI and CALIOP altitude over oceanic regions, CALIOP being the reference. In addition to the overall correlation already seen, if this diagram shows overall amplitude similar to that of CALIOP (0.91), it also shows a large dispersion of the amplitudes for the sites. Among the "Level 2" sites with a mean AOD
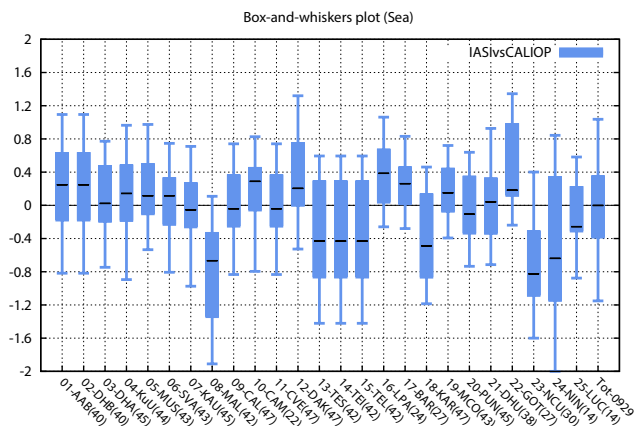
Figure 7. Box-and-whiskers plot (ends of the whiskers exclude the outliers) for the difference between IASI and CALIOP altitude over oceanic regions. y axis is in kilometres. Sites are identified by their number and code as defined in Table 4, followed by the number of items. Last box: overall result. NB: a systematic bias of -0.4 km (IASI–CALIOP) has been removed from the mean (all sites and total).

larger than 0.08, amplitudes that are much too small are observed for the three sites at Tenerife(13–15), overlapping with an amplitude of ~ 0.60 and a correlation of ~ 0.63, and for Karachi(18). Amplitudes that are too large are observed for Dakar(12), Abu_Al_Bukhoosh(1), and Dhabi(2). Sites with a mean AOD less than 0.08 generally show poor results. Again, we see that the method cannot be applied to low-AOD situations. The box-and-whiskers plot for the difference between IASI and CALIOP altitude – first and third quartiles and median – over oceanic regions is shown in Fig. 7. In this figure, the difference between the median and 0 is the bias observed between IASI and CALIOP. Here, a systematic bias of -0.4 km (IASI–CALIOP) has been removed. The overall standard deviation is 0.48 km, explained in part by the layering of the radiative transfer code used to compute the LUTs: two adjacent layers are separated by ~ 0.85 km. For the overall sample, there is no skewness and an inner quartile range (third quartile minus first quartile) of ~ 0.8 km. Most sites show a small skewness with the exception (again) of CRPSM_Malindi(8), Camaguey(10), Dakar(12), and GOT_Seaprism(22). Lucinda(25) again shows strange behaviour. Largest remaining biases, seen in Fig. 7 (-0.4 km, giving a total bias of -0.8 km), are observed for the three Tenerife sites. These results over oceanic regions must be improved; they demonstrate that the difficulties met in determining the AOD are largely amplified when determining the altitude.

For a majority of sites over land, essentially over deserts, results for altitude are not satisfactory. To the reasons discussed above for the AOD must be added the lower sensitivity of IASI to altitude. Work is in progress to solve these difficulties.

4.3 Impact of the refractive index in the infrared

While numerous measurements of the aerosol refractive index (real and imaginary parts) actually exist in the visible part of the spectrum, this is not the case in the infrared. However, refractive indices in the infrared are often marked by a relatively large spectral variability from one source of aerosol to another. Sokolik et al. (1998) illustrate this variability well, listing most of the existing measurements of mineral aerosol infrared refractive index. This can cause important changes in the aerosol optical characteristics (Sokolik et al., 1998; Claquin et al., 1998; Sokolik and Toon, 1999; Pierangelo, 2013) and, consequently, in the dust radiative forcing, both in the infrared and in the visible. Figure A2 of the Appendix shows infrared refractive indices from four sources: the MITR model from the OPAC data base (Hess et al., 1998), resulting from the measurements by Volz (1973) and representative of desert dust far from the sources; the "dust-like" model from the measurements by Volz (1972, 1973), more representative of non desert mineral aerosols generated from soil; the "revisited" index, proposed by Balkanski et al. (2007) in an effort to reevaluate mineral aerosol radiative forcings; and the "Volz-Fouquart" model from Saharan dust measurements above Niger (Volz cited by Fouquart et al., 1987). At this stage, it is worth pointing out that, in the infrared, the impact of the refractive model is difficult to quantify a priori since it depends on the variability of both its imaginary and real parts at the central wavelengths of *all* the channels used in the retrieval process (Pierangelo et al., 2004). Locations of the IASI channels used in the present approach are shown by the vertical bars in Fig. A2. Because this study was carried out using a single refractive index model (the MITR model) whatever the location of the site considered, it appeared important to test the sensitivity of the results to a change in the refractive index. IASI results have thus been reevaluated using the "revisited" mineral dust refractive index (Balkanski et al., 2007), which shows significant differences with the MITR model, in particular around 9.3, 11.5, or 11.8 μm, as illustrated by Fig. A2.

With this new refractive index model, new LUTs have been computed and the whole retrieval process has been redone. Figure 8 summarizes the differences found between the MITR evaluation and this new evaluation for the sites over land (see Table 3). This figure shows differences, site by site and total, between MITR and "revisited" for the correlation (red) and the amplitude (blue) for the AOD (IASI versus AERONET). Positive (negative) values mean better correlation and an amplitude closer to 1 for MITR ("revisited"). A few conclusions stand out from this comparison. Concerning the correlation, there are four differences larger than 0.10. Two support the use of MITR: Dakar(6) with a difference of 0.12 and Gual_Pahari(15) with a difference of 0.15 and too low a number of items to really be significant; two support the use of the "revisited" IR refractive indices: Ilorin(11) with a difference of 0.11 and Kanpur(16)
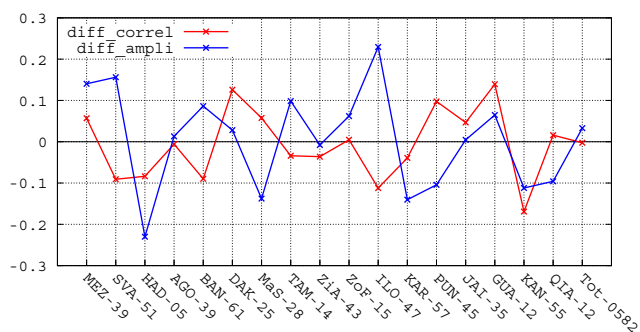
Figure 8. Differences, site by site and total ("Tot"), found between the MITR and "revisited" evaluations (see Sect. 4.3) for the AOD (IASI versus AERONET) and for the sites over land (see Table 3). Differences in correlation are shown in red; differences in amplitude (normalized standard deviation) are shown in blue. Positive (negative) values mean better correlation and an amplitude closer to 1 for MITR ("revisited").

with a difference of 0.17; the latter site is under the influence of the Thar desert, the primary potential source of dusts in the Indian subcontinent (Dey et al., 2004, and references therein). Differences in amplitude are clearer with three sites that support the use of MITR (Mezaira(1), Solar_Village(2), and Ilorin(11)), and four sites that support the use of "revisited" (DMN_Maine_Soroa(7), Karachi(12), Pune(13), and Kanpur(16)). Some sites show larger correlation but smaller amplitude, contrary, for example, to Kanpur with the two results that support the use of "revisited". Concerning the box-and-whiskers results, we have observed that differences in the median are negligible and that differences in the inner quartile range are slightly more important, the three largest differences (however, less than 0.04) supporting the use of "revisited".

These results show the significant impact of this change in refractive index model for some sites and the relevance of the Sokolik et al. (1998) recommendation regarding the use of a particular refractive index according to the geographical region considered. Differences between the two experiments made here are significant and point to the need of more new experimental measurements. As detailed in Appendix A, they would be even more significant with the "dust-like" or the "Fouquart" refractive index models as they differ more from the MITR model than the "revisited" model does.

4.4 AOD and altitude time series

Time series of the AOD from IASI and AERONET and of the altitude from IASI and CALIOP give another view of the degree of agreement between the different sources of the products. They also highlight the frequent lack of AERONET data throughout the period of study. Lack of IASI data is also seen, due to not enough IASI daily results in the monthly average (presence of persistent clouds, rejection by the algorithm, etc.). Because of the relatively large number of sites

considered in this study, we present the time series figures in the Supplement associated with this paper.

Figure S1 in the Supplement shows time series of the 10 μm IASI AOD (red) and of the AERONET coarse-mode 500 nm AOD (black) for the sites over oceanic regions. AERONET AOD is scaled by the empirical IR / Vis coarse-mode AOD site ratio, determined as explained in Sect. 3, and shown at the top left of each figure. Figure S2 in the Supplement shows similar time series for the sites over land. Several remarks can be made about these figures. A relatively modest result seen from the Taylor diagrams can result from low AOD (for example, at CRPSM_Malindi(8), Lucinda(25), GOT_Seaprism(22)). A good correlation can mask an IR / Vis ratio a priori far from its theoretical value: a ratio of 2.3 is obtained at Izana(14), the site elevation (2400 m) of which is problematic when compared to IASI, which integrates the whole atmospheric column. For the same site, the difference between the amplitudes of the IASI and the AERONET time series is obvious; as already said, an anomalous ratio can mask a bias of the IASI AOD. Similar remarks can be made for the sites over land. Similar remarks can be made for the sites over land, for example, the smaller amplitudes of the IASI time series for Mezaira(1), Agoufou(4), Banizoumbou(5), DMN_Maine_Soroa(7), Zinder_Airport(9), and Zouerate_Fennec(10), however all "Level 1.5" sites, except the first one. The same time series also show that the IASI AOD is likely too high outside the aerosol season. Incidentally, the largest IASI AOD ever observed in this study, ∼ 0.7, is for Qiandaohu(17) over land. There are no AERONET measurements for this event (December 2008), but one exists for the nearby site of LA_TM (119.40° E, 30.32° N). Fig. S3 shows the corresponding AOD time series, which confirm the IASI observation for this event. Figure S4 in the Supplement shows time series of the IASI (red) and CALIOP (green) altitude (km) for the sites over oceanic regions. The most obvious remark is the (expected) difficulty of deriving altitude in case of weak AOD (see, for example, CRPSM_Malindi(8), or EPA_NCU(23)). Also, there are several amplitude problems (Tenerife sites (13–15), Karachi(18), etc.) or phase shifts (Calhau(9), Capo_Verde(11), etc.), illustrating that improving the method is still necessary.

5 Discussion and conclusions

5.1 AOD

In this study, IASI-derived dust AOD has been evaluated using AERONET ground-based measurements of the 500 nm coarse-mode AOD for 38 sites (of which four sites are considered both over oceanic regions and land) of the tropical band. There are sites over oceanic regions, over land, and over desert. Most sites are of AERONET quality "Level 2"

(quality-assured), the rest being of quality "Level 1.5", meaning that they have been cloud-screened but may not have final calibration applied. The evaluation method relies on the analysis of Taylor diagrams and of box-and-whiskers plots. To overcome the difficulty raised by the difference between the two spectral domains used to derive the AOD, and hence different metrics, a fit is done, site by site, including all the available items for the period studied, resulting in an IASI IR (10 µm) / AERONET Vis (500 nm) AOD "empirical" coarse-mode site ratio. Theory (see Appendix A for details) shows that this ratio essentially depends on the refractive index (in particular its infrared part, which is measured much less than its visible part), on the width of the size distribution, and on the effective radius, the latter two being given, but not always, at each AERONET site. With these parameters varying from one site to another (and, often, from one day to the next), there is no one common factor reconciling the two observation metrics. For sites over oceanic regions, we infer a mean ratio of 0.79 ± 0.25; a lower mean ratio is obtained over land: 0.55 ± 0.15. Although these values are compatible with theoretical simulations, the dispersion is significant and comes not only from the variability, site by site, of the influencing variables, but also from the possibly incorrect use of the MITR aerosol model for a particular site. As shown in Sect. 3 and Appendix A, theoretical values of this ratio vary from 1.1, using the MITR refractive index model, to 0.4, using models more representative of aerosols closer to sources. The problem raised by the determination of an "empirical" coarse-mode site ratio is that of a bias potentially affecting the IASI AOD: in that case, the procedure will mask the bias and produce a wrong empirical site ratio. Large differences in the amplitudes of the IASI and scaled AERONET AOD time series, as well as degraded correlations, are potential signs of such a problem. Also, if too few items are available over the time period studied, the fit may not really be representative of the whole seasonal cycle and hence may lead to an incorrect ratio: the smaller the number of items, the less reliable the results. In general, results are significantly better over oceanic regions, where surface characteristics (temperature, emissivity) are more accurately retrieved, than over land, particularly in case of heterogeneous terrains.

Over oceanic regions, the main results found for the AOD in this work are (i) a strong overall correlation of 0.86 between IASI and AERONET monthly mean AOD for the 786 items representing all the months available at the 25 sites; (ii) weaker correlations observed for some sites with complex aerosol situations marked by the influence of a variety of sources, or for some sites that may reasonably be suspected not to correspond to the MITR model used here (Hess et al., 1998); (iii) overall amplitude (normalized standard deviation) similar to that of AERONET; and (iv) no skewness of the overall sample (as well as of most site samples) and a relatively small inner quartile range of ~ 0.05.

Over land, the overall correlation comes to 0.74 for the 582 items representing all the months available at the 17 sites.

This is a relatively high correlation, keeping in mind that, here, the proportion of "Level 1.5" sites is larger (47 %) than over oceanic regions (32 %). All sites show smaller amplitude than that of the reference AERONET (amplitude of 0.86 for the overall sample), with a stronger discrepancy found over Sahara, where most sites are "Level 1.5". In addition to the explanations already given for sites over oceanic regions, pronounced terrain heterogeneities, increasing the difficulty of determining surface characteristics (emissivity and temperature; see Capelle et al., 2012), have a negative impact on the AOD accuracy. The box-and-whiskers diagram over land (Fig. 5) shows results that are significantly degraded compared to the ones over the oceans (Fig. 3) with a majority of skewed distributions.

5.2 Altitude

With 929 items for the whole period (all sites over oceanic regions), the overall correlation is 0.65 and the overall amplitude is 0.91. Eliminating three sites – CRPSM_Malindi(10), due to too low a mean AOD (0.04), Ningbo(24) and Lucinda(25), due to too low a number of items (14) – gives a correlation of 0.7 for 853 items (overall amplitude: 0.92). This is significantly worse than for the AOD but still acceptable. Actually, a correlation weaker than for the AOD was expected, due to the great difference between the two approaches (definition of the altitude, difference in the space–time resolutions, and lower sensitivity of IASI to altitude than to AOD). It is also seen that low IASI AODs increase the difficulty of determining the altitude from IASI. The Taylor diagram that depicts the altitude of the dust layer over the oceans (Fig. 6) shows overall amplitude similar to that of AERONET and also shows a large dispersion in the site amplitudes. There is a systematic bias of -0.4 km between IASI and CALIOP (IASI–CALIOP). The box-and-whiskers plot (Fig. 7, in which the systematic bias has been removed) for the overall sample shows a small skewness and a relatively small inner quartile range (third quartile minus first quartile) of ~ 0.55 km. Most sites show no pronounced skewness. Results over land, particularly over deserts, are not satisfactory. We suggest that this is due to terrain heterogeneities and elevation as well as to the residual presence of dust aerosols in the lower troposphere. Work is in progress to solve these difficulties.

5.3 Problem of the refractive index

One of the limits of the present approach is the systematic use of the MITR refractive index model. The experiment consisting of exchanging this model for the "revisited" IR refractive indices from Balkanski et al. (2007) and proceeding to a new evaluation has provided some indications concerning the sensitivity of such an evaluation to the refractive index model used in the inversion. First, it highlights the significant impact of this change in refractive index model for certain

sites: two sites (one) show a better correlation with "revisited" (MITR); four sites (three) show a better amplitude with "revisited" (MITR). Second, it confirms the relevance of the Sokolik et al. (1998) recommendations regarding the use of refractive index adapted to the geographical region considered. For example, Highwood et al. (2003), analysing infrared interferometric measurements made during the Saharan Dust Experiment (SHADE), get the best agreement when using the "Fouquart" refractive index model. This highlights the need for more new experimental measurements of refractive indices for more geographical aerosol source regions. Recent publications by Journet et al. (2014) and by Di Biagio et al. (2014) seem promising. The method used here to derive aerosol characteristics from IASI can be applied immediately to such new measurements.

5.4 Difficulties of the evaluation

The evaluation as described above encounters several problems. First, the number of IASI–AERONET monthly mean AOD bins per site is often much smaller than the number of months of the period studied (72). The most complete site is, by far, Capo_Verde, with 65 items. The overall mean is ~ 33, with large variations, and the time distribution is not always representative of the seasonal cycle. Second, measuring either in the visible or in the infrared, AERONET and IASI do not share the same AOD metrics. The fit used to adapt the AERONET metrics to that of IASI must be made site by site due to the dependence of the infrared to visible AOD coarse-mode ratio on the refractive index, the size distribution, and the effective radius, all varying from one site to another. A wrong empirical ratio may result from the incorrect use of the MITR model for a particular site, from the presence of IASI AOD biases, or from a fit with too small a number of items. Wrong site ratios should, in principle, correspond to differences in the amplitude of the IASI and AERONET AOD time series, as well as to degraded correlations. However, as shown in the Appendix, it is interesting to point out that, despite its limited accuracy, the "empirical" IR / Vis AOD coarse-mode ratio, directly determined by the ratio of the IASI-retrieved 10 µm AOD and the AERONET 500 nm coarse-mode AOD, can be interpreted as a *marker* of the aerosol situation observed. Over land, and particularly over desert, terrain heterogeneities may render the determination of the surface characteristics more problematic, resulting in a degradation of the dust properties derived from IASI. Moreover, the episodic presence of dust within the lower troposphere, particularly for sites close to active sources (Sahara, for example), to which IASI is poorly sensitive, contrary to AERONET, may also lead to differences between ground-based AERONET observations and IASI retrievals. Finally, the level of IASI radiometric noise at short wavelengths hampers the altitude retrieval, the quality of which relies on a combination of long-wave and shortwave channels (Pierangelo et al., 2004; Peyridieu et al., 2013).

In spite of these difficulties, the overall agreement between IASI and AERONET for the AOD and between IASI and CALIOP for the altitude is satisfactory. AERONET, CALIOP, and IASI all have their advantages and drawbacks: the present results demonstrate the usefulness of IASI data, which are designed to cover a long period of time, as an additional constraint to a better knowledge of the impact of aerosols on the climate system. With the aim of a still more accurate comparison between IASI and AERONET, work is in progress to analyse IASI results on a daily scale, over the tropics as well as over midlatitudes. Preliminary results, in particular over the Mediterranean Sea, are encouraging.
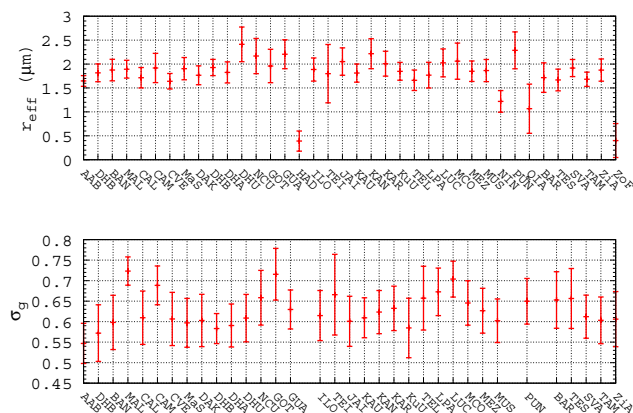
Figure A1. Mean values (±one standard deviation) of r_{eff} and σ_{g} for the 38 AERONET sites analysed in this study (see Table 1). The standard deviation associated with each site corresponds to the variability of the parameter considered over the whole time period analysed (July 2007–June 2013).

Appendix A: Impact of dust aerosol microphysical properties on the IR / VIS AOD coarse-mode ratio and on IASI brightness temperatures

The parameters describing aerosol optical properties are the extinction coefficient, directly linked to the AOD; the single scattering albedo; and the asymmetry parameter. These parameters enter the radiative transfer equation for computing radiances or brightness temperatures (BT), a quantity commonly used in the infrared. These optical properties may be obtained from the a priori knowledge of the aerosol microphysical properties (size distribution and effective radius, refractive indices) using a Lorenz–Mie algorithm (e.g. Mishchenko et al., 2002). With the purpose of comparing infrared (10 μm) AOD to visible (500 nm) coarse-mode AOD, the size distribution can be modelled by a monomodal log-normal distribution (see, for example, Zender et al., 2002 and Dubovik et al., 2002) that is described by the effective radius (r_{eff}) and the standard deviation of the distribution σ_{g}. In the following, σ_{g} stands for $\ln(\sigma_{\mathrm{g}})$. This approximation is justified by the fact that, if we only consider the dust coarse-mode, the contribution of the fine mode in the long-wave domain is less than 10 % (Pierangelo et al., 2013, Sect. 9).

In this appendix, we investigate the variability of dust aerosol microphysical properties and their impact on the IR / VIS AOD coarse-mode ratio and on the IASI brightness temperatures.
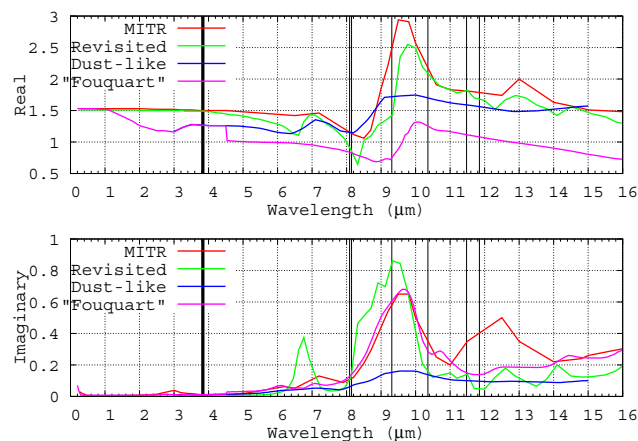

Figure A2. Real (top) and imaginary (bottom) refractive index for the MITR model (Hess et al., 1998; Volz, 1973) in red; the "revisited" (Balkanski et al., 2007) model in green; the "dust-like" model from Volz (1972, 1973) in blue, and "Fouquart" et al. (1987) in pink. Black vertical bars indicate the location of the IASI channels used in the aerosol retrieval.

A1 Range of variation of the dust aerosol microphysical properties

A1.1 Size distribution parameters (from AERONET)

For each of the 38 sites analysed in this study, Fig. A1 shows the mean, ±one standard deviation, of r_{eff} (top) and of σ_{g} (bottom) as provided by the AERONET archive for the coarse mode. The standard deviation at each site corresponds to the variability of the parameter considered over the whole time period July 2007–June 2013. From this figure, the ranges of variation of r_{eff} and σ_{g} are, respectively, 1.5–2.5 μm and 0.5–0.8 (a few sites, with too few items, have not been taken into account). This figure also shows the relatively low variability of the site-by-site mean value of r_{eff} and, to a lesser extent, of σ_{g}.

A1.2 Refractive index

Unlike the size distribution parameters, the infrared part of the refractive index is not available from the AERONET archive. However, the aerosol composition is variable and may change during transport (see for example Highwood et al., 2003), inducing a change in the refractive index from one place to the other. The impact of the refractive index on the IR / VIS AOD coarse-mode ratio and on IASI brightness temperatures has been investigated for four models: MITR (see Sect. 2.1); "revisited", proposed by Balkanski et al. (2007), in an effort to re-evaluate mineral aerosol radiative forcings; "dust-like", from the measurements by Volz (1972, 1973), more representative of non-desert mineral aerosols generated from soil; and "Fouquart", from Saharan dust measurements
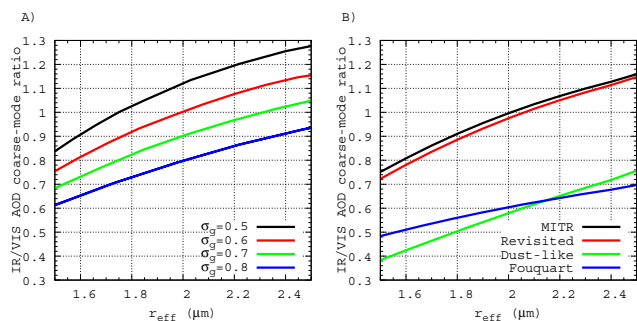
Figure A3. Theoretical IR / Vis AOD coarse-mode ratio as a function of the effective radius **(a)** for the MITR model and the standard deviation of the width of the size distribution σ, **(b)** for $\sigma = 0.6$ and several refractive indices.

above Niger (from Volz, cited by Fouquart et al., 1987), representative of dust above sources. Figure A2 displays the real and imaginary parts of the refractive index for these four models. In this figure, black vertical bars indicate the location of the IASI channels used in the aerosol retrieval.

A2 Sensitivity of the IR / VIS AOD coarse-mode ratio to microphysical parameters

Figure A3a displays the values of the theoretical IR / Vis AOD coarse-mode ratio for typical values of σ_g (0.5–0.8) and r_{eff} (1.5–2.5 µm) found in the AERONET database for the 38 sites selected and for the MITR refractive index. It is seen that the IR / Vis AOD coarse-mode ratio can vary within quite a large range: 0.6–1.3. Figure A3b displays the values taken by this ratio for the four refractive index models of Fig. A2 and typical values of r_{eff} (here, $\sigma_g = 0.6$). Two model pairs behave similarly: on the one hand, MITR and "revisited", more representatives of aerosols far from sources, and, on the other hand, "dust-like" and "Fouquart", more representatives of aerosols closer to sources. The range of variation is, again, quite large: 0.4–1.15. Moreover, once σ_g and r_{eff} are given, the impact of the refractive index on the ratio can reach 40 % if the ratio is estimated with a refractive index more typical of aerosols close or far from dust sources. For example, with $r_{eff} = 1.8$ µm and $\sigma_g = 0.65$, the ratio may go from ~ 0.55 to ~ 0.90 (Fig. A3b).

For this evaluation of IASI-derived aerosol characteristics around AERONET sites, for which the standard deviation of the size distribution and the effective radius are provided, this analysis demonstrates that the crucial parameter, governing the conversion of the AOD from the visible domain to the infrared domain, is the refractive index, substantially varying with the type of aerosol considered. Unfortunately, an obvious lack of measurements of dust refractive index in the infrared precludes determining an accurate theoretical IR / Vis AOD coarse-mode site ratio.
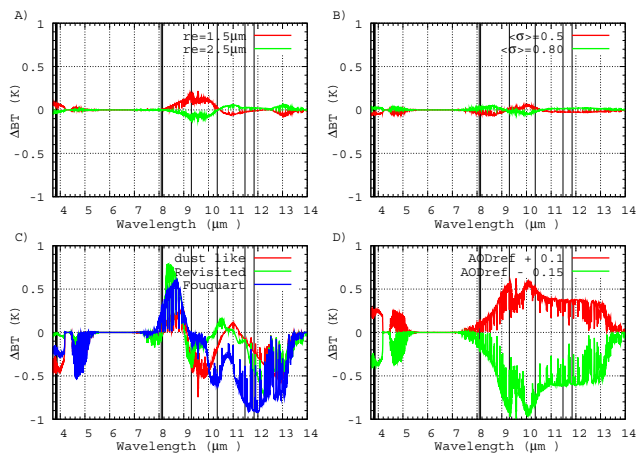

Figure A4. Sensitivity of IASI brightness temperature to **(a)** a variation of ± 25 % of the effective radius r_{eff} (designated r_e in the diagram); **(b)** a variation of ± 25 % of the standard deviation σ_g; **(c)** a change in the refractive index (i.e. composition); **(d)** an AOD variation of $+0.1$ (~ 25 %) and -0.15 (~ -37 %). Reference conditions: AOD at 10 µm = 0.4, mean aerosol layer altitude = 2700 m, $r_{eff} = 2$ µm, $\sigma_g = 0.65$, and refractive index is MITR.

A3 Sensitivity of the infrared brightness temperature (BT) to microphysical parameters

In order to quantify the impact of microphysical parameters on infrared brightness temperatures, difference in BT to a reference case is computed for a relatively high AOD of 0.4 at 10 µm and for an aerosol layer at a mean altitude of 2700 m. The reference configuration corresponds to the averaged values seen in the AERONET database: $\sigma_g = 0.65$, $r_{eff} = 2$ µm, refractive index model: MITR (from Volz et al., 1973, slightly modified by Carlson and Benjamin, 1980). Figure A4 shows the sensitivity of the IASI brightness temperature to a variation of ± 25 % of the effective radius r_{eff} **(a)**, a variation of ± 25 % of the standard deviation σ_g **(b)**, a change of the refractive index **(c)**, and a variation of the AOD **(d)**.

Concerning the variation of r_{eff} (Fig. 4a), maximum differences are smaller than 0.2 K for an AOD of 0.4 at 10 µm. Note that the impact is proportional to the AOD: because the AOD is generally not larger than 0.6 at 10 µm, the maximum impact is less than 0.5 K for the channel the most sensitive to the size (at 9.3 µm). Indeed, for the channels used in the retrieval, the impact is less than 0.3 K for an AOD of 0.6. We conclude that, in the infrared domain, the effect of the effective radius is small, particularly on the channels selected. This agrees with Sokolik et al. (1998). Concerning σ_g, the impact is less than 0.1 K over the entire infrared spectrum, quite negligible compared to the impact of a variation in AOD (see also, e.g., Pierangelo et al. (2013), Sect. 9.4). Similar results are obtained for a reference (extreme) 10 µm AOD of 0.6 (impact of 0.2 K instead of 0.1). Finally, the impact

of the refractive index is, by far, the most important. For an AOD of 0.4, the difference in BT can reach 0.8 K for two of the channels used in the retrieval (around $12\,\mu m$–$830\,cm^{-1}$). To summarize, for the "reference case" used in this appendix ($\sigma_g = 0.65$, $r_{eff} = 2\,\mu m$), using OPAC instead of "Fouquart" can lead to an error of 0.1 for an AOD of 0.4, i.e. a 25 % error. At the same time, the variation of the theoretical IR / Vis ratio will reach 40 %. This large signal means that, despite its limited accuracy, the "empirical" IR / Vis ratio, directly determined by the ratio of the IASI-retrieved $10\,\mu m$ AOD and the AERONET $500\,nm$ coarse-mode AOD, can be interpreted as a *marker* of the aerosol situation observed. Actually, as shown in Sect. 4.1.1, the mean empirical ratio comes to 0.79 ± 0.25 for the sites over oceanic regions, which are far from sources and for which MITR is best adapted, and to 0.55 ± 0.15 for the sites over land, which are closer to sources and for which the "Fouquart" model is best adapted, following Highwood et al. (2003). This result gives some confidence in the value of this empirical ratio.

The publication of this article is financed by CNRS-INSUs.

References

Amiridis, V., Wandinger, U., Marinou, E., Giannakaki, E., Tsekeri, A., Basart, S., Kazadzis, S., Gkikas, A., Taylor, M., Baldasano, J., and Ansmann, A.: Optimizing CALIPSO Saharan dust retrievals, Atmos. Chem. Phys., 13, 12089–12106, doi:10.5194/acp-13-12089-2013, 2013.

Balkanski, Y., Schulz, M., Claquin, T., and Guibert, S.: Reevaluation of Mineral aerosol radiative forcings suggests a better agreement with satellite and AERONET data, Atmos. Chem. Phys., 7, 81–95, doi:10.5194/acp-7-81-2007, 2007.

Basart, S., Pérez, C., Cuevas, E., Baldasano, J. M., and Gobbi, G. P.: Aerosol characterization in Northern Africa, Northeastern Atlantic, Mediterranean Basin and Middle East from direct-sun AERONET observations, Atmos. Chem. Phys., 9, 8265–8282, doi:10.5194/acp-9-8265-2009, 2009.

Capelle, V., Chédin, A., Péquignot, E.,Schlüssel, P., Newman, S. M., and Scott, N. A.: Infrared continental surface emissivity spectra and skin temperature retrieved from IASI observations over the tropics, J. Appl. Meteor. Climatol., 51, 1164–1179, doi:10.1175/JAMC-D-11-0145.1, 2012.

Chalon, G., Cayla, F., and Diebel, D.: IASI: An Advanced Sounder for Operational Meteorology, Proceedings of the 52nd Congress of IAF, Toulouse France, October, 2001.

Chiapello, I., Bergametti, G., Gomes, L., Chatenet, B., Dulac, F., Pimenta, J., and Santos Suares, E.: An additional low layer transport of Sahelian and Saharan dust over the North-Eastern Tropical Atlantic, Geophys. Res. Lett., 22, 3191–3194, 1995.

Chiapello, I., Moulin, C., and Prospero, J. M.: Understanding the long-term variability of African dust transport across the Atlantic as recorded in both Barbados surface concentrations and large-scale Total Ozone Mapping Spectrometer (TOMS) optical thickness, J. Geophys. Res., 110, D18S10, doi:10.1029/2004JD005132, 2005.

Claquin, T., Schulz, M., Balkanski, Y., and Boucher, O.: Uncertainties in assessing radiative forcing by mineral dust, Tellus B, 50, 491–505, 1998.

De Souza-Machado, S., Strow, L. L., Motteler, H., and Hannon, S.: Infrared dust spectral signatures from AIRS, Geophys. Res. Lett., 33, L03801, doi:10.1029/2005GL024364, 2006.

Dey, S., Tripathi, S. N., Singh, R. P., and Holben, B. N.: Influence of dust storms on the aerosol optical properties over the Indo-Gangetic basin, J. Geophys. Res., 109, D20211, doi:10.1029/2004JD004924, 2004.

Di Biagio, C., Boucher, H., Caquineau, S., Chevaillier, S., Cuesta, J., and Formenti, P.: Variability of the infrared complex refractive index of African mineral dust: experimental estimation and implications for radiative transfer and satellite remote sensing, Atmos. Chem. Phys. Discuss., 14, 10597–10657, doi:10.5194/acpd-14-10597-2014, 2014.

Eck, T. F., Holben, B. N., Dubovik, O., Smirnov, A., Slutsker, I., Lobert, J. M., and Ramanathan, V.: Column-integrated aerosol optical properties over the Maldives during the northeast monsoon for 1998–2000, J. Geophys. Res., 106, 28555–28566, 2001.

Eck, T. F., Holben, B. N., Reid J. S., Sinyuk, A., Dubovik, O., Smirnov, A., Giles, D., O'Neill, N. T., Tsay, S.-C., Ji, Q., Al Mandoos, A., Ramzan Khan, M., Reid, E. A., Schafer, J. S., Sorokine, M., Newcomb, W., and Slutsker, I.: Spatial and temporal variability of column-integrated aerosol optical properties in the southern Arabian Gulf and United Arab Emirates in summer, J. Geophys. Res., 113, D01204, doi:10.1029/2007JD008944, 2008.

Eck, T. F., Holben, B. N., Sinyuk, A., Pinker, R. T., Goloub, P., Chen, H., Chatenet, B., Li, Z., Singh, R. P., Tripathi, S. N., Reid, J. S., Giles, D. M., Dubovik, O., O'Neill, N. T., Smirnov, A., Wang, P., and Xia, X.: Climatological aspects of the optical properties of fine/coarse mode aerosol mixtures, J. Geophys. Res., 115, D19205, doi:10.1029/2010JD014002, 2010.

Formenti, P., Schütz, L., Balkanski, Y., Desboeufs, K., Ebert, M., Kandler, K., Petzold, A., Scheuvens, D., Weinbruch, S., and Zhang, D.: Recent progress in understanding physical and chemical properties of African and Asian mineral dust, Atmos. Chem. Phys., 11, 8231–8256, doi:10.5194/acp-11-8231-2011, 2011.

Forster, P., Ramaswamy, V., Artaxo, P., Berntsen, T., Betts, R., Fahey, D. W., Haywood, J., Lean, J., Lowe, D. C., Myhre, G., Nganga, J., Prinn, R., Raga, G., Schulz, M., and Van Dorland, R.: Radiative Forcing of Climate Change, in: Climate Change 2007: The Physical Science Basis. Contribution of Working Group I to the Fourth Assessment Report of the Intergovernmental Panel on Climate Change, edited by: Solomon, S., Qin, D., Manning, M., Chen, Z., Marquis, M., Averyt, K. B., Tignor, M., and Miller, H. L., 129–234, Cambridge Univ. Press, Cambridge, UK and New York, NY, USA, 2007.

Hansen, J., Sato, M., and Ruedy, R.: Radiative forcing and climate response, J. Geophys. Res., 102, 6831–6864, doi:10.1029/96JD03436, 1997.

Haywood, J. M. and Ramaswamy, V.: Global sensitivity studies of the direct radiative forcing due to anthropogenic sulfate and black carbon aerosols, J. Geophys. Res., 103, 6043–6058, doi:10.1029/97JD03426, 1998.

Hess, M., Koepke, P., and Schult, I.: Optical Properties of Aerosols and Clouds: The software package OPAC, B. Am. Meteorol. Soc., 79, 831–844, 1998.

Highwood, E., Haywood, J. M., Silverstone, M. D., Newman, S. M., and Taylor, J. P.: Radiative properties and direct effect of Saharan dust measured by the C-130 aircraft during Saharan Dust Experiment (SHADE), 2. Terrestrial spectrum, J. Geophys. Res., 108, 8578, doi:10.1029/2002JD002 552, 2003.

Holben, B. N., Eck, T. F., Slutsker, I., Tanre, D., Buis, J. P., Setzer, A., Vermote, E., Reagan, J. A., Kaufman, Y. J., Nakajima, T., Lavenu, F., Jankowiak, I., and Smirnov, A.: AERONET – A federated instrument network and data archive for aerosol characterization, Remote Sens. Environ., 66, 1–16, 1998.

Huneeus, N., Schulz, M., Balkanski, Y., Griesfeller, J., Prospero, J., Kinne, S., Bauer, S., Boucher, O., Chin, M., Dentener, F., Diehl, T., Easter, R., Fillmore, D., Ghan, S., Ginoux, P., Grini, A., Horowitz, L., Koch, D., Krol, M. C., Landing, W., Liu, X., Mahowald, N., Miller, R., Morcrette, J.-J., Myhre, G., Penner, J., Perlwitz, J., Stier, P., Takemura, T., and Zender, C. S.: Global dust model intercomparison in AeroCom phase I, Atmos. Chem. Phys., 11, 7781–7816, doi:10.5194/acp-11-7781-2011, 2011.

Journet, E., Balkanski, Y., and Harrison, S. P.: A new data set of soil mineralogy for dust-cycle modeling, Atmos. Chem. Phys., 14, 3801–3816, doi:10.5194/acp-14-3801-2014, 2014.

Kalashnikova, O. V. and Kahn, R. A.: Mineral dust plume evolution over the Atlantic from MISR and MODIS aerosol retrievals, J. Geophys. Res., 113, D24204, doi:10.1029/2008JD010083, 2008.

Kaskaoutis, D. G., Kalapureddy, M. C. R., Krishna Moorthy, K., Devara, P. C. S., Nastos, P. T., Kosmopoulos, P. G., and Kambezidis, H. D.: Heterogeneity in pre-monsoon aerosol types over the Arabian Sea deduced from ship-borne measurements of spectral AODs, Atmos. Chem. Phys., 10, 4893–4908, doi:10.5194/acp-10-4893-2010, 2010.

Kaufman, Y. J., Tanre, D., Gordon, H. R., Nakajima, T., Lenoble, J., Frouin, R., Grassl, H., Hermann, B. M., King, M. D., and Teillet, P. M.: Passive remote sensing of tropospheric aerosol and atmospheric correction for the aerosol effect, J. Geophys. Res., 102, 16815–16830, doi:10.1029/97JD01496, 1997.

Klüser, L., Martynenko, D., and Holzer-Popp, T.: Thermal infrared remote sensing of mineral dust over land and ocean: a spectral SVD based retrieval approach for IASI, Atmos. Meas. Tech., 4, 757–773, doi:10.5194/amt-4-757-2011, 2011.

Klüser, L., Kleiber, P., Holzer-Popp, T., and Grassian, V. H.: Desert dust observation from space – Application of measured mineral component infrared extinction spectra, Atmos. Environ., 54, 419–427, 2012.

Knippertz, P. and Todd, M. C.: Mineral dust aerosols over the Sahara: Meteorological controls on emission and transport and implications for modeling, Rev. Geophys., 50, RG1007, doi:10.1029/2011RG000362, 2012.

Kocha, C., Tulet, P., Lafore, J.-P., and Flamant, C.: The importance of the diurnal cycle of Aerosol Optical Depth in West Africa, Geophys. Res. Lett., 40, 785–790, doi:10.1002/grl.50143, 2013.

Koepke, P., Hess, M., Schult, I., and Shettle, E. P.: Global aerosol data set, Rep. No. 243, Max-Planck Institut für Meteorologie, Hamburg, Germany, 44 pp., 1997.

Legrand, M, Bertrand, J. J., Desbois, M., Menenger L., and Fouquart, Y.: The potential of infrared satellite data for the retrieval of saharan-dust optical depth over Africa, J. Appl. Meteorol., 28–24, 309–319, doi:10.1175/15200450, 1989.

Léon, J.-F. and Legrand, M.: Mineral dust sources in the surroundings of the north Indian Ocean, Geophys. Res. Lett., 30, 1309, doi:10.1029/2002GL016690, 2003.

Ma, X., Bartlett, K., Harmon, K., and Yu, F.: Comparison of AOD between CALIPSO and MODIS: significant differences over major dust and biomass burning regions, Atmos. Meas. Tech., 6, 2391–2401, doi:10.5194/amt-6-2391-2013, 2013.

Maher, B. A., Prospero, J. M., Mackie, D., Gaiero, D., Hesse, P. P., and Balkanski, Y.: Global connections between aeolian dust, climate and ocean biogeochemistry at the present day and at the last glacial maximum, Earth-Sci. Rev., 99, 61–97, doi:10.1016/j.earscirev.2009.12.001, 2010.

Mahowald, N. M., Kloster, S., Engelstaedter, S., Moore, J. K., Mukhopadhyay, S., McConnell, J. R., Albani, S., Doney, S. C., Bhattacharya, A., Curran, M. A. J., Flanner, M. G., Hoffman, F. M., Lawrence, D. M., Lindsay, K., Mayewski, P. A., Neff, J., Rothenberg, D., Thomas, E., Thornton, P. E., and Zender, C. S.: Observed 20th century desert dust variability: impact on climate and biogeochemistry, Atmos. Chem. Phys., 10, 10875–10893, doi:10.5194/acp-10-10875-2010, 2010.

Markowicz, K. M., Flatau, P. J., Vogelmann, A. M., Quinn, P. M., and Welton, E.: Influence of relative humidity on aerosol radiative forcing: An ACE-Asia experiment perspective. J. Geophys. Res., 108, 8662, doi:10.1029/2002JD003066, 2003.

Mishchenko, M. I., Travis, L. D., and Lacis, A. A.: Scattering, Absorption, and Emission of Light by Small Particles, Cambridge University Press, Cambridge, 2002.

Müller, D., Lee, K.-H., Gasteiger, J., Tesche, M., Weinzierl, B., Kandler, K., Müller, T., Toledano, C., Otto, S., Althausen, D., and Ansmann, A.: Comparison of optical and microphysical properties of pure Saharan mineral dust observed with AERONET Sun photometer, Raman lidar, and in situ instruments during SAMUM 2006, J. Geophys. Res., 117, D07211, doi:10.1029/2011JD016825, 2012.

Myhre, G. and Stordal, F.: Global sensitivity experiments of the radiative forcing due to mineral aerosols, J. Geophys. Res., 106, 18193–18204, 2001.

Omar, A. H., Winker D. M., Tackett J. L., Giles D. M., Kar J., Liu Z., Vaughan M. A., Powell K. A., and Trepte C. R.: CALIOP and AERONET aerosol optical depth comparisons: One size fits none, J. Geophys. Res.-Atmos., 118, 4748–4766, doi:10.1002/jgrd.50330, 2013.

O'Neill, N. T., Eck, T. F., Smirnov, A., Holben, B. N., and Thulasiraman, S.: Spectral discrimination of coarse and fine mode optical depth, J. Geophys. Res., 108, 4559, doi:10.1029/2002JD002975, 2003.

Otto, S., de Reus, M., Trautmann, T., Thomas, A., Wendisch, M., and Borrmann, S.: Atmospheric radiative effects of an in situ measured Saharan dust plume and the role of large particles, Atmos. Chem. Phys., 7, 4887–4903, doi:10.5194/acp-7-4887-2007, 2007.

Peyridieu, S., Chédin, A., Tanré, D., Capelle, V., Pierangelo, C., Lamquin, N., and Armante, R.: Saharan dust infrared optical depth and altitude retrieved from AIRS: a focus over North Atlantic – comparison to MODIS and CALIPSO, Atmos. Chem. Phys., 10, 1953–1967, doi:10.5194/acp-10-1953-2010, 2010.

Peyridieu, S., Chédin, A., Capelle, V., Tsamalis, C., Pierangelo, C., Armante, R., Crevoisier, C., Crépeau, L., Siméon, M., Ducos, F., and Scott, N. A.: Characterisation of dust aerosols in the infrared from IASI and comparison with PARASOL, MODIS, MISR, CALIOP, and AERONET observations, Atmos. Chem. Phys., 13, 6065–6082, doi:10.5194/acp-13-6065-2013, 2013.

Pierangelo, C., Chédin, A., Heilliette, S., Jacquinet-Husson, N., and Armante, R.: Dust altitude and infrared optical depth from AIRS, Atmos. Chem. Phys., 4, 1813–1822, doi:10.5194/acp-4-1813-2004, 2004.

Pierangelo, C., Mishchenko, M., Balkanski, Y., and Chédin, A.: Retrieving the effective radius of Saharan dust coarse mode from AIRS, Geophys. Res. Lett., 32, L20813, doi:10.1029/2005GL023425, 2005.

Pierangelo, C.: in: Aerosol Remote Sensing, edited by: Lenoble, J., Remer, L., and Tanré, D., Chap. 9, Springer-Praxis Books: Environmental Sciences, 510 pp., ISBN-13: 9783642174407, 2013.

Reid, J. S., Piketh, S. J., R. Kahn, R., Bruintjes, R. T., and Holben, B. N.: A Summary of First Year Activities of the United Arab Emirates Unified Aerosol Experiment: UAE2, Naval Research Laboratory report nb. NRL/MR/7534–05-8899, 150 pp., 2005.

Reid, J. S., Piketh, S. J. , Walker, A. L. , Burger, R. P. , Ross, K. E. , Westphal, D. L. , Bruintjes, R. T. , Holben, B. N. , Hsu, N. C. , Jensen, T. L. , Kahn, R. A. , Kuciauskas, A. P. , Mandoos, A. Al, Mangoosh, A. Al , Miller, S. D. , Porter, J. N. , Reid, E. A., and Tsay, S. C.: An overview of UAE2 flight operations: Observations of summertime atmospheric thermodynamic and aerosol profiles of the southern Arabian Gulf, J. Geophys. Res., 113, D14213, doi:10.1029/2007JD009435, 2008.

Ryder, C. L., Highwood, E. J., Rosenberg, P. D., Trembath, J., Brooke, J. K., Bart, M., Dean, A., Crosier, J., Dorsey, J., Brindley, H., Banks, J., Marsham, J. H., McQuaid, J. B., Sodemann, H., and Washington, R.: Optical properties of Saharan dust aerosol and contribution from the coarse mode as measured during the Fennec 2011 aircraft campaign, Atmos. Chem. Phys., 13, 303–325, doi:10.5194/acp-13-303-2013, 2013.

Scott, N. A. and Chédin, A.: A fast line-by-line method for atmospheric absorption computations: The Automatized Atmospheric Absorption Atlas, J. Appl. Meteor., 20, 802–812, 1981.

Shao, Y., Wyrwoll, K., Chappell, A., Huang, J., Lin, Z., McTainsh, G. H., Mikami, M., Tanaka, T. Y., Wang, X., and Yoon, S.: Dust cycle: An emerging core theme in Earth system science, Aeolian Res., 2, 181–204, doi:10.1016/j.aeolia.2011.02.001, 2011.

Singh, R. P., Dey, S., Tripathi, S. N., Tare, V., and Holben, B.: Variability of aerosol parameters over Kanpur, northern India, J. Geophys. Res., 109, D23206, doi:10.1029/2004JD004966, 2004.

Smirnov, A., Holben, B. N., Dubovik, O., O'Neill, N. T., Eck, T. F., Westphal, D. L., Goroch, A. K., Pietras, C., and Slutsker, I.: Atmospheric Aerosol Optical Properties in the Persian Gulf, J. Atm. Sci., 59, 620–634, 2002.

Sokolik, I. N. and Toon, O. B.: Incorporation of mineralogical composition into models of the radiative properties of mineral aerosol from UV to IR wavelengths, J. Geophys. Res., 104, 9423–9444, 1999.

Sokolik, I., Toon, O. B., and Bergstrom, R.W.: Modeling the radiative characteristics of airborne mineral aerosols at infrared wavelengths, J. Geophys. Res., 103, 8813–8826, 1998.

Stamnes, K., Tsay, S.-C., Wiscombe, W., and Jayaweera, K.: Numerically stable algorithm for discrete ordinate-method radiative transfer in multiple scattering and emitting layered media, Appl. Optics, 27, 2502–2509, 1988.

Tanré, D., Haywood, J., Pelon, J., Léon, J.-F., Chatenet, B., Formenti, P., Francis, P., Goloub, P., Highwood, E., and Myhre, G.: Measurement and modeling of the Saharan dust radiative impact: Overview of the Saharan Dust Experiment (SHADE), J. Geophys. Res., 108, 8574, doi:10.1029/2002JD003273, 2003.

Taylor, K. E.: Summarizing multiple aspects of model performance in a single diagram, J. Geophys. Res., 106, 7183–7192, 2001.

Tesche, M., Wandinger, U., Ansmann, A., Althausen, D., Muller, D., and Omar, A. H.: Ground-based validation of CALIPSO observations of dust and smoke in the Cape Verde region, J. Geophys. Res. Atmos., 118, 2889–2902, doi:10.1002/jgrd.50248, 2013.

Tsamalis, C., Chédin, A., Pelon, J., and Capelle, V.: The seasonal vertical distribution of the Saharan Air Layer and its modulation by the wind, Atmos. Chem. Phys., 13, 11235–11257, doi:10.5194/acp-13-11235-2013, 2013.

US Climate Change Science Program: Atmospheric aerosol properties and climate impacts, A report by the U.S. Climate Change Science Program and the Subcommittee on Global Change Research, edited b:y Chin, M., Kahn, R. A., and Schwartz, S. E., report, 128 pp., NASA, Washington, D. C., 2009.

Vogelmann, A. M., Flatau, P. J., Szczodrak, M., Markowicz, K. M., and Minnett, P. J.: Observations of large aerosol infrared forcing at the surface, Geophys. Res. Lett., 30, 1655, doi:10.1029/2002GL016829, 2003.

Volz, F. E.: Infrared Refractive Index of Atmospheric Aerosol Substances, Appl. Opt., 11, 755–759, 1972.

Volz, F. E.: Infrared optical constants ammonium sulfate, Sahara dust, volcanic pumace and flyash, Appl. Opt., 12, 564–568, 1973.

Walters Sr., K. R. and Sjoberg, W. F.: The Persian Gulf Region, A Climatological Study, US Marine Corps, p. 62, available at: http://www.marines.mil/News/Publications/ELECTRONICLIBRARY/ElectronicLibraryDisplay/tabid/13082/Article/127213/fmfrp-0-54.aspx, 1990.

Wang, S. H., Lin, N. H., Chou, M. D., Tsay, S. C., Welton, E. J., Hsu, N. C., Giles, D. M., Liu, G. R., and Holben, B. N.: Profiling transboundary aerosols over Taiwan and assessing their radiative effects, J. Geophys. Res., 115, D00K31, doi:10.1029/2009JD013798, 2010.

Winker, D., Hunt, W., and McGill, M.: Initial performance assessment of CALIOP, Geophys. Res. Lett., 34, L19803, doi:10.1029/2007GL030135, 2007.

Winker, D. M., Vaughan, M. A., Omar, A. H., Hu, Y., Powell,K. A., Liu, Z., Hunt, W. H., and Young, S. A.: Overview of the CALIPSO Mission and CALIOP Data Processing Algorithms, J. Atmos. Oceanic Technol., 26, 2310–2323, doi:10.1175/2009JTECHA1281.1, 2009.

Winker, D. M., Pelon, J., Coakley Jr., J. A., Ackerman, S. A., Charlson, R. J., Colargo, P. R., Flamant, P., Fu, Q., Hoff, R. M., Kittaka, C., Kubar, T. L., Le Treut, H., McCormick, M. P., Mégie, G., Poole, L., Powell, K., Trepte, C., Vaughan, M. A., and Wielicki, B. A.: The CALIPSO Mission: A Global 3D View of Aerosols and Clouds, B. Am. Meteorol. Soc., 91, 1211–1229, doi:10.1175/2010BAMS3009.1, 2010.

Yu, H., Kaufman, Y. J., Chin, M., Feingold, G., Remer, L. A., Anderson, T. L., Balkanski, Y., Bellouin, N., Boucher, O., Christopher, S., DeCola, P., Kahn, R., Koch, D., Loeb, N., Reddy, M. S., Schulz, M., Takemura, T., and Zhou, M.: A review of measurement-based assessments of the aerosol direct radiative effect and forcing, Atmos. Chem. Phys., 6, 613–666, doi:10.5194/acp-6-613-2006, 2006.